AD-A123 997 OSCILLATOR STRENGTHS FOR THE VIBRATIONAL INDUCED ELECTRIC-DIPOLE TRANSITIONS IN CS2NARCI6(U) HARRY DIAMOND LABS ADELPHI MD C A MORRISON ET AL. DEC 82 1/1

UNCLASSIFIED HDL-TR-2000 F/G 20/12 NL

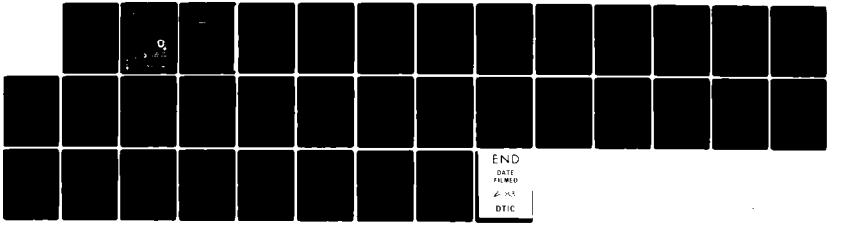

END

DATE FILMED

4-83

DTIC

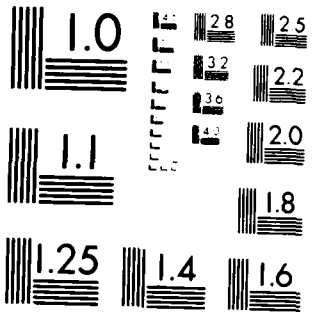

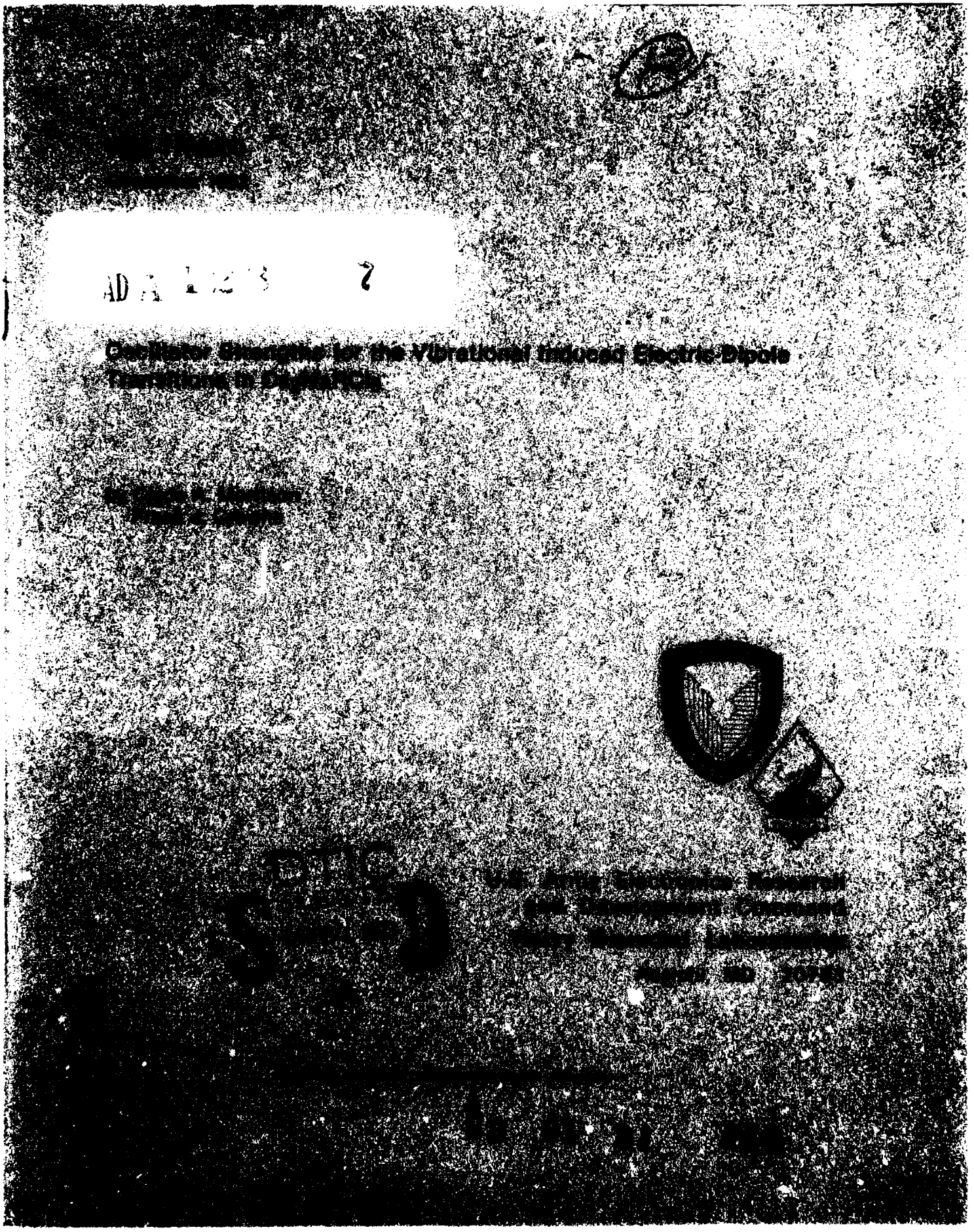
AD
Oscillator Strengths for the Vibrational Induced Electric-Dipole
Transitions in Diatomics
DTIC

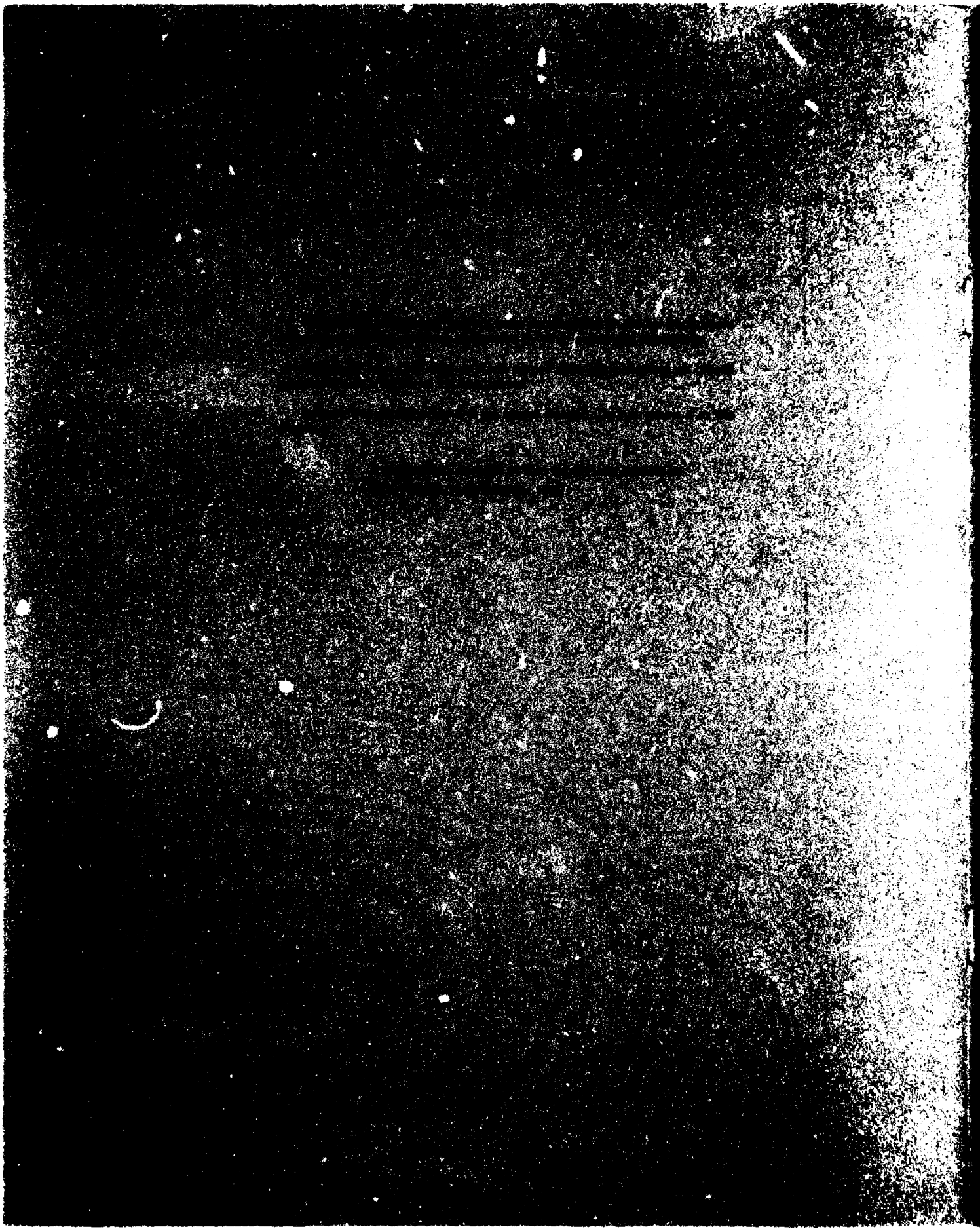

UNCLASSIFIED

SECURITY CLASSIFICATION OF THIS PAGE (When Data Entered)

REPORT DOCUMENTATION PAGE

READ INSTRUCTIONS BEFORE COMPLETING FORM

1. REPORT NUMBER: HDL-TR-2000

2. GOVT ACCESSION NO.: AD-A123 997

3. RECIPIENT'S CATALOG NUMBER:

4. TITLE (and Subtitle): Oscillator Strengths for the Vibrational Induced Electric Dipole Transitions in Cs_2NaRCl_6

5. TYPE OF REPORT & PERIOD COVERED: Technical Report

6. PERFORMING ORG. REPORT NUMBER:

7. AUTHOR(s):
Clyde A. Morrison
Frank J. Crowne

8. CONTRACT OR GRANT NUMBER(s):

9. PERFORMING ORGANIZATION NAME AND ADDRESS:
Harry Diamond Laboratories
2800 Powder Mill Road
Adelphi, MD 20783

10. PROGRAM ELEMENT, PROJECT, TASK AREA & WORK UNIT NUMBERS:
Program Ele: 61102A
DA Project: 1L161102A31B

11. CONTROLLING OFFICE NAME AND ADDRESS:
Night Vision and Electro-Optics Laboratory
Fort Belvoir, VA 22060

12. REPORT DATE: December 1982

13. NUMBER OF PAGES: 35

14. MONITORING AGENCY NAME & ADDRESS (if different from Controlling Office):

15. SECURITY CLASS. (of this report): UNCLASSIFIED

15a. DECLASSIFICATION/DOWNGRADING SCHEDULE:

16. DISTRIBUTION STATEMENT (of this Report):
Approved for public release; distribution unlimited.

17. DISTRIBUTION STATEMENT (of the abstract entered in Block 20, if different from Report):

18. SUPPLEMENTARY NOTES:
HDL Project: 319232
DRCMS Code: 61110231B0011

19. KEY WORDS (Continue on reverse side if necessary and identify by block number):
Phonons
Vibronics
Rare-earth ions
Spectra

20. ABSTRACT (Continue on reverse side if necessary and identify by block number):
The vibrational modes of the elpasolite structure Cs_2NaRCl_6 are discussed in detail. The interaction potential of the rare-earth ion substituted at the R site is developed for multipolar charge distribution on the ligand (Cl) site. The theory is used to calculate the vibronic transition intensity for the ν_6 (87 cm^{-1}) mode for Er in $Cs_2NaErCl_6$. The results indicate that the strength of the vibronic transition from the $^4I_{15/2} \rightarrow {}^4F_{9/2}$ is approximately the same as the strength of the magnetic-dipole transitions. The vibronic line strength for transitions to the other multiplets was, in general, less than the corresponding magnetic-dipole transitions.

DD FORM 1 JAN 73 1473 EDITION OF 1 NOV 65 IS OBSOLETE

UNCLASSIFIED

SECURITY CLASSIFICATION OF THIS PAGE (When Data Entered)

CONTENTS

FIGURES

TABLES

1. INTRODUCTION

The recent development of various kinds of tunable solid-state lasers[1-3]* has revitalized interest in electronic-vibrational (vibronic) transitions of impurity ions in solids; in particular, laser action on phonon-terminated transitions, predicted by McCumber,[4] has been realized. A thorough understanding of the mechanism of these phonon-terminated lasers can and should lead to the development of a useful and versatile class of lasers that operate at shorter and at longer wavelengths than do presently existing systems.

The mechanism for vibrationally induced electric-dipole transitions for transition-metal ions at a site with inversion symmetry in a solid was discussed by Van Vleck[5] as early as 1937; however, serious investigations into the order of magnitude of vibronic electric-dipole transitions did not begin until the 1950's. During this latter period, a large number of papers were written invoking vibronics in the analysis of transition-metal ions with an unfilled d shell. Of these papers, the work of Liehr and Ballhausen[6,7] purported to be the most complete, although from our standpoint a further discussion of details would have been helpful. An early paper by Koide and Pryce[8] has been, by far, the most useful to us in our efforts.

Simultaneously with intense research efforts on the role of vibronics in the behavior of transition-metal ions, some work was also begun on the rare-earth series. In two papers,[9-10] Satten discussed the effects of vibronics on electric-dipole transitions and the Zeeman splittings of rare-earth ions in solids and solutions. Also, Pollock and Satten[11] and Satten et al[12] extended the analysis to actinide ions as well as rare-earth ions. Much of the latter work relied very heavily on group-theoretical methods in the development, in order to extract the symmetry dependence very concisely. Much of this analysis was applied to cases where the ions under investigation occupied sites of low symmetry or cubic sites in solids where charge compensation is required (for example, triply ionized rare-earth ions in CaF_2).

The discovery[13] of the elpasolite hexachlorides, Cs_2NaRCl_6 with R any of the triply ionized rare-earth ions, changed the experimental situation. It was found that Cs_2NaRCl_6 of good optical quality could be grown with R any rare earth, or with R = Y and a small amount of rare earth added. The site occupied by R^{3+} in Cs_2NaRCl_6 has O_h symmetry, and the resulting spectra are rich in vibronics.[14] Because of the sharpness of the rare-earth spectra, a large number of different vibrational modes can be identified, and by fitting the frequencies of these modes a

Because of their large number, literature references are listed at the end of the text rather than on each page.

number of force constants in the vibrational Hamiltonian can be determined.[15] The determination of these force constants allows a quantitative calculation of the intensity of the vibrationally induced electric-dipole transitions. Such a calculation has been performed by Hasan and Richardson,[16] whose theoretical predictions were found to be in rough agreement with experiment. These calculations are important for possible technical applications[17] of this material or the less hygroscopic, isomorphic compounds Cs_2NaRF_6 and Rb_2NaRF_6. Unfortunately, very few of the vibronic spectra of the latter, more practical compounds have been reported. Nevertheless, an analysis of vibronics of Er^{3+} in Cs_2NaRCl_6 should be very useful.

In this report, we investigate the electric-dipole transitions of Er^{3+} in $Cs_2NaErCl_6$ caused by the odd vibrations of the $(RCl_6)^{-3}$ complex. Most of the results will be presented in a form that allows simple generalization to the complete unit cell (in the $k \approx 0$ limit), although this generalization will necessarily involve the use of a computer. Thus, the analysis of the normal modes of the complete unit cell such as given by Lentz[18] can be readily used in any future calculations. In section 2, we discuss the modes of vibration of the $(RCl_6)^{-3}$ ion. In section 3, the static crystal field is discussed using the point-charge, point-multipole potential model. Also in section 3, the self-induced crystal field of Faulkner and Richardson[19] is presented in a slightly different form generalized from dipoles to multipoles.[20] The vibrational electronic interaction is the subject of section 4, along with an explicit calculation of the electric-dipole transitions for Er^{3+} accompanying the ν_6 vibration of $(ErCl_6)^{-3}$.

2. VIBRATIONAL MODES OF $(RCl_6)^{-3}$

The ion cores that make up the crystal and determine the crystal field felt by an electron on a rare-earth ion are located at sites in the crystal which are local minima of the effective ion-core potential; i.e., each ion is in its own potential well. It is well known that these ions can execute small vibrations within their wells, and that for small amplitudes of vibration each ion behaves like a harmonic oscillator. The interionic forces will in general couple these oscillators, so that the crystal as a whole has extended wave-like normal modes which, for an infinite crystal, can be characterized by a wave number, k. When these modes are quantized, their quanta make up the elementary excitations of the background crystal--the so-called phonons.

The normal modes of a typical crystal fall into two categories:

(1) Acoustic modes: these are characterized by all the atoms of a unit cell moving at once in nearly the same direction by nearly the same amount. Every crystal has three such modes.

(2) Optical modes: these modes involve some countermotion of atoms in the unit cell; if there are N atoms in the unit cell, there are N - 3 optical modes.

In general, acoustic modes correspond at low values of k to crystal strain waves, and involve macroscopic motion of the crystal bulk; their frequencies $\omega(k)$ cover a rather broad band in k-space: from k = 0 to k on the order of a reciprocal lattice vector, $\omega(k)$ may vary by as much as 100 meV. By contrast, the optical modes are always microscopic motions which do not give rise to bulk movement of the crystal matrix; their frequencies tend to be narrow band (~5 meV) due to the rather weak coupling of adjacent unit cells that execute this kind of motion.[21] Because the form of the crystal field is intimately related to the unit cell configuration, the motions associated with these two kinds of normal modes will have radically different effects on the electronic states of a rare-earth ion.

In dealing with a crystal with a complicated unit cell like elpasolite, it pays to examine the crystal vibrations from a molecular standpoint. This entails the following simplified picture of the ion motion:

(1) Acoustic modes correspond to simple translation of every ion in the cell, and have zero frequency.

(2) Optical modes do not couple one unit cell to another.

Clearly this picture is simply one of a single unit cell hanging in space, and being treated like an isolated molecule. We expect that this picture will be fairly good for those normal modes which are self-contained, i.e., those for which the boundary atoms of the cell are motionless. Actually, it turns out to be good for all the optical modes, with three glaring exceptions: an isolated unit cell has three rotational modes with zero frequency which go into nonzero frequency optical modes that will clearly couple the unit cells together in a nontrivial way.

In figure 1 we show the full unit cell of elpasolite. In general, a full normal-mode analysis of the optical modes of this crystal reveals that one need only specify the motion of the atom in the primitive unit cell, and that translation operators will give the motion of the remaining atoms. These essential atoms (from a vibrational standpoint) are shown in figure 2, taken from a paper by Lentz.[18] The basic vibrating structure consists of a pair of octahedra joined at a vertex, flanked by two cesium atoms. It is clear that if a rare earth is placed at the center of one of these octahedra, the normal modes which couple most strongly to it are those which correspond to the vibrations of the free octahedral complex.

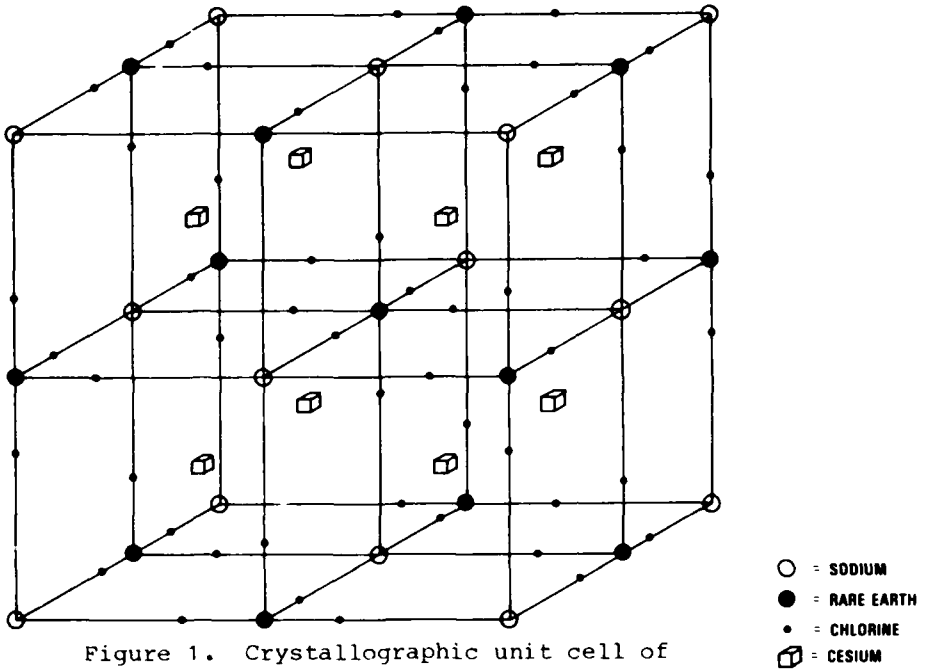

Figure 1. Crystallographic unit cell of Cs_2NaRCl_6.

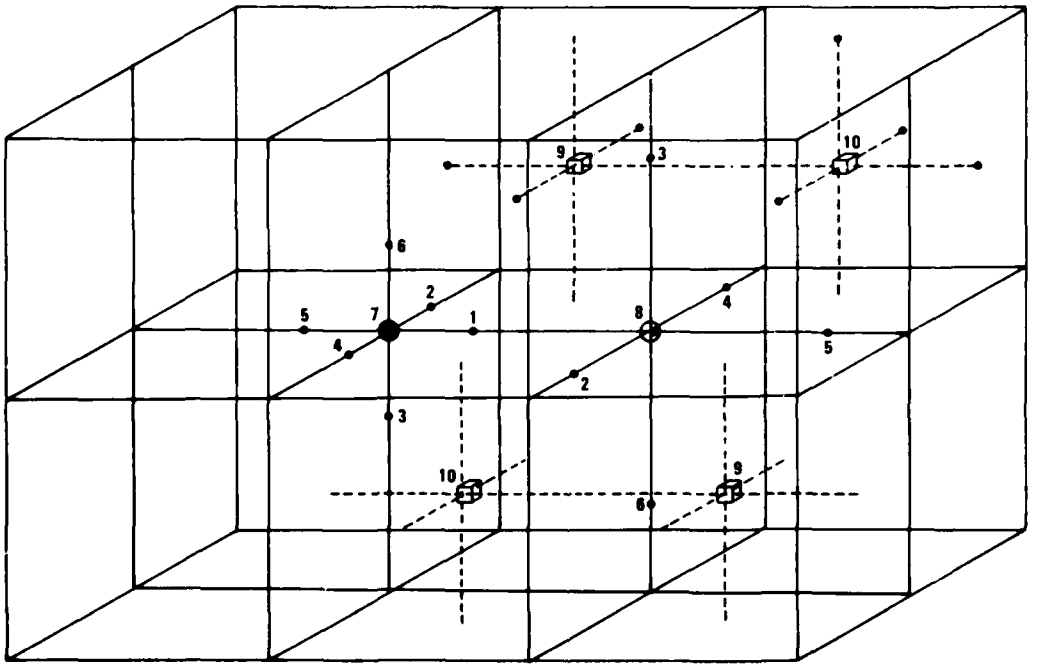

Figure 2. Vibrational unit cell (after ref 18; equivalent atoms have the same labels).

The normal modes of a free octahedron have been known for some time.[8] In figure 2 we show an octahedron; labeling the atomic displacement coordinates (x_N, y_N, z_N), N = 1, . . . 7, we see that there are 21 degrees of freedom, and hence 21 normal modes. A group-theoretic analysis reveals that these 21 modes, which form a representation of the O_h group, can be grouped by symmetry into the following irreducible representations of O_h:

$$\Gamma_1^+(a_{1g}) \quad ,$$

$$\Gamma_3^+(e_{1g}) \quad ,$$

$$\Gamma_4^+(t_{1g}) \quad ,$$

$$3\Gamma_4^-(t_{1u}) \quad ,$$

$$\Gamma_5^-(t_{2u}) \quad ,$$

$$\Gamma_5^+(t_{2g}) \quad .$$

Of these representations, the t_{1g} and one of the t_{1u} modes correspond to the zero-frequency rotation and translation modes, respectively.

Now, there exist sets of so-called "symmetry coordinates," i.e., linear combinations of the (x_N, y_N, z_N), which reduce the classical vibrational Hamiltonian to block form: by this we mean that the symmetry coordinates transform as irreducible representations of O_h. If a given irreducible representation appears once in the regular representation generated by the ion coordinates (x_N, y_N, z_N), then the corresponding symmetry coordinate is a normal mode. In general, however, the regular representation may contain a given irreducible representation several times; in this case, there will be several symmetry coordinates associated with the ion coordinates, none of which is a normal mode. In this case, the symmetry coordinates do not fully diagonalize the Hamiltonian, and the true normal coordinates are linear combinations of symmetry coordinates of a given irreducible representation.

The problem of a free vibrating octahedral complex illustrates everything we have discussed thus far. Figure 3 shows the labeling system that we will use here. Figure 4 shows the eight "symmetry vibrations" of an octahedron with a rare-earth ion at its center, corresponding to the appropriate symmetry coordinates; if the actual ion coordinates (the six chlorine ions plus the rare earth) are labeled (x_N, y_N, z_N), then in terms of these coordinates the symmetry coordinates are as follows:

(A) Translation: $\Gamma_4^-(t_{1u})$

$$\tau_1 = \eta^2 x_7 + \zeta^2(x_1 + x_2 + x_3 + x_4 + x_5 + x_6) \ ,$$

$$\tau_2 = \eta^2 y_7 + \zeta^2(y_1 + y_2 + y_3 + y_4 + y_5 + y_6) \ ,$$

$$\tau_3 = \eta^2 z_7 + \zeta^2(z_1 + z_2 + z_3 + z_4 + z_5 + z_6) \ ,$$

where

$$\zeta = (6 + \varepsilon^2)^{-1/2} \ ,$$

$$\varepsilon = \sqrt{M_0/M} \ ,$$

$$\eta = \varepsilon\zeta \ ,$$

M_0 is the rare-earth mass, and

M is the ligand (i.e., chlorine) mass.

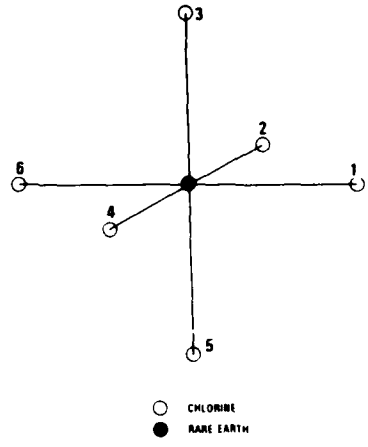

Figure 3. Labeling for RCl_6 octahedron.

Note that the τ_i are simply the center-of-mass coordinates of the octahedral complex.

(B) Rotation: $\Gamma_4^+(t_{1g})$

$$\rho_1 = \frac{\zeta}{2}(z_2 - z_4 + y_5 - y_3) \ ,$$

$$\rho_2 = \frac{\zeta}{2}(z_6 - z_1 + x_3 - x_5) \ ,$$

$$\rho_3 = \frac{\zeta}{2}(x_4 - x_2 + y_1 - y_6) \ .$$

(C) "Breather:" $\Gamma_1^+(a_{1g})$

$$\Delta = \frac{\zeta}{\sqrt{6}}(x_1 - x_6 + y_2 - y_4 + z_3 - z_5) \ .$$

(D) Doublet: $\Gamma_3^+(e_{1g})$

$$\sigma_1 = \frac{\zeta}{2\sqrt{3}}[2(x_1 - x_6) - (y_2 - y_4) - (z_3 - z_5)] \ ,$$

$$\sigma_2 = \frac{\zeta}{2\sqrt{3}}[2(z_3 - z_5) - (x_1 - x_6) - (y_2 - y_4)] \ .$$

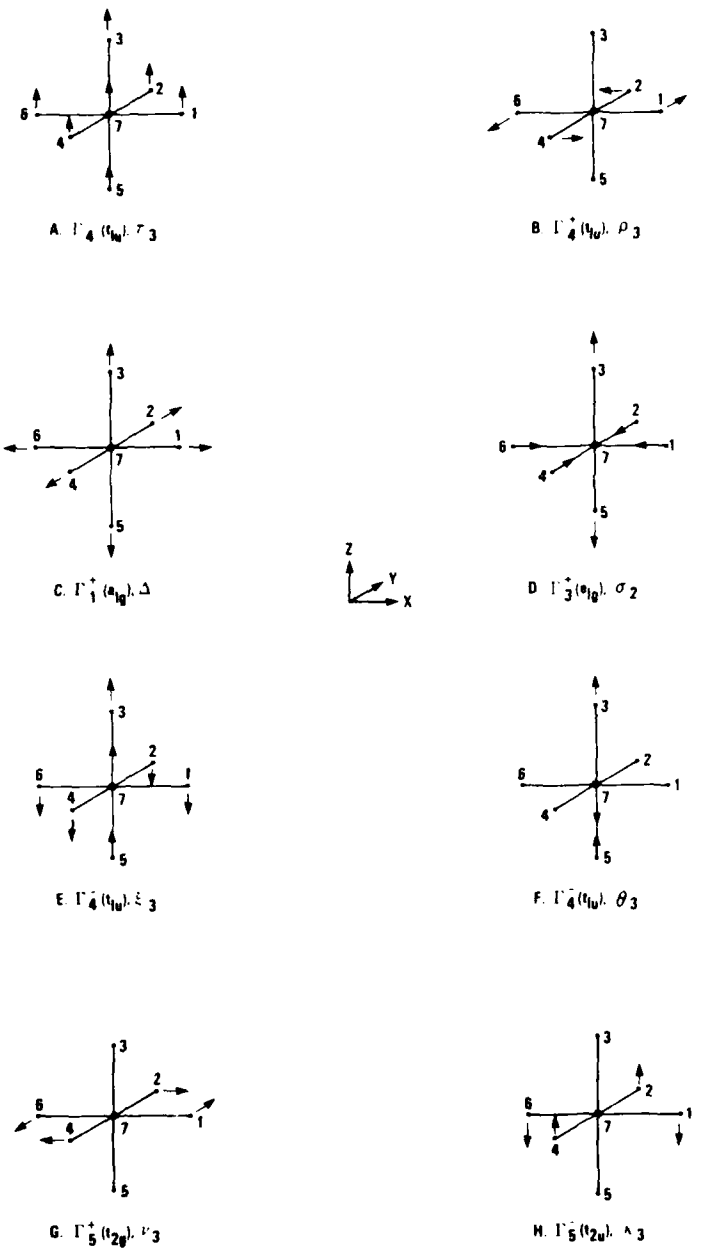

Figure 4. Normal modes of an octahedron, with corresponding symmetry coordinates.

(E) $\Gamma_4^-(t_{1u})$

$$\xi_1 = \alpha x_7 + \beta(x_1 + x_6) - \gamma(x_2 + x_3 + x_4 + x_5) \quad ,$$

$$\xi_2 = \alpha y_7 + \beta(y_2 + y_4) - \gamma(y_1 + y_3 + y_5 + y_6) \quad ,$$

$$\xi_3 = \alpha z_7 + \beta(z_3 + z_5) - \gamma(z_1 + z_2 + z_4 + z_6) \quad ,$$

where

$$\alpha = 2\eta^2 / \sqrt{\varepsilon^2 + 2} \quad ,$$

$$\beta = 2\zeta^2 / \sqrt{\varepsilon^2 + 2} \quad ,$$

$$\gamma = \frac{1}{2}\zeta^2 \sqrt{\varepsilon^2 + 2} \quad ,$$

(F) $\Gamma_4^-(t_{1u})$

$$\theta_1 = \lambda x_7 - \mu(x_1 + x_6) \quad ,$$

$$\theta_2 = \lambda y_7 - \mu(y_2 + y_4) \quad ,$$

$$\theta_3 = \lambda z_7 - \mu(z_3 + z_5) \quad ,$$

where

$$\lambda = \varepsilon\zeta\sqrt{\frac{2}{2 + \varepsilon^2}} \quad ,$$

$$\mu = \frac{1}{2}\lambda \quad .$$

(G) $\Gamma_5^+(t_{2g})$

$$\nu_1 = \frac{\zeta}{2}(y_5 - y_3 + z_4 - z_2) \quad ,$$

$$\nu_2 = \frac{\zeta}{2}(z_1 - z_6 + x_3 - x_5) \quad ,$$

$$\nu_3 = \frac{\zeta}{2}(y_1 - y_6 + x_2 - x_4) \quad .$$

(H) $\Gamma_5^-(t_{2u})$

$$\kappa_1 = \frac{\zeta}{2}(x_2 + x_4 - x_5 - x_3) \quad ,$$

$$\kappa_2 = \frac{\zeta}{2}(y_1 + y_6 - y_3 - y_5) \quad ,$$

$$\kappa_3 = \frac{\zeta}{2}(z_2 + z_4 - z_1 - z_6) \quad .$$

If we write the classical Hamiltonian in terms of these eight symmetry coordinates (with their appropriate conjugate momenta), it is completely diagonal except for a term

$$H^1 = (\vec{\theta}^+, \vec{\xi}^+) \begin{pmatrix} V_{11} & V_{12} \\ V_{21} & V_{22} \end{pmatrix} \begin{pmatrix} \vec{\theta} \\ \vec{\xi} \end{pmatrix} .$$

This term is not diagonal because $\vec{\theta}$ and $\vec{\xi}$ both transform like $\Gamma_4^-(t_{1u})$. The normal modes depend on the values of V_{ij}, which in turn relate to the specific forces between the octahedron's constituents.

If we now want to consider the effect these vibrations have on the crystal field experienced by the octahedron's center, we clearly need to know the detailed motion of each ion when a given normal mode is excited. In quantum mechanical language, there are phonons associated with each normal mode; the motion of an electron will cause emission and absorption of these phonons, and these phonons in turn act back on the electron. The interaction potential will be derived in section 4; for now, we note that it will involve the ion coordinates themselves, *not* the normal modes. In order to evaluate the various transition probabilities, we must therefore express the ion coordinates in terms of the normal modes; i.e., we must invert relations (A) to (H). Once this is done, we must subtract off the rare-earth coordinate, since the electron is "*riding with*" the rare earth. When this is done, the following results obtain: if $\Delta x_i = x_i - x_7$, $\Delta y_i = y_i - y_7$, and $\Delta z_i = z_i - z_7$, then

$$\Delta x_1 = -A\theta_1 + \frac{1}{\zeta}\left(\frac{1}{\sqrt{6}}\Delta + \frac{1}{\sqrt{3}}\sigma_1\right) ,$$

$$\Delta y_1 = -B\xi_2 - C\theta_2 + \frac{1}{2\zeta}\left(\kappa_2 + \rho_3 + \nu_3\right) ,$$

$$\Delta z_1 = -B\xi_3 - C\theta_3 + \frac{1}{2\zeta}\left(-\kappa_3 - \rho_2 + \nu_2\right) ;$$

$$\Delta x_2 = -B\xi_1 - C\theta_1 + \frac{1}{2\zeta}\left(\kappa_1 - \rho_3 + \nu_3\right) ,$$

$$\Delta y_2 = -A\theta_2 + \frac{1}{\zeta}\left(\frac{1}{\sqrt{6}}\Delta - \frac{1}{\sqrt{3}}\left(\sigma_1 + \sigma_2\right)\right) ,$$

$$\Delta z_2 = -B\xi_3 - C\theta_3 + \frac{1}{2\zeta}\left(\kappa_3 + \rho_1 - \nu_1\right) ;$$

$$\Delta x_3 = -B\xi_1 - C\theta_1 + \frac{1}{2\zeta}\left(-\kappa_1 + \rho_2 + \nu_2\right) \quad ,$$

$$\Delta y_3 = -B\xi_2 - C\theta_2 + \frac{1}{2\zeta}\left(-\kappa_2 - \rho_1 - \nu_1\right) \quad ,$$

$$\Delta z_3 = -A\theta_3 + \frac{1}{\zeta}\left(\frac{1}{\sqrt{6}}\,\Delta - \frac{1}{\sqrt{3}}\,\sigma_2\right) \quad ;$$

$$\Delta x_4 = -B\xi_1 - C\theta_1 + \frac{1}{2\zeta}\left(\kappa_1 + \rho_3 - \nu_3\right) \quad ,$$

$$\Delta y_4 = -A\theta_2 + \frac{1}{\zeta}\left(-\frac{1}{\sqrt{6}}\,\Delta + \frac{1}{\sqrt{3}}\left(\sigma_1 + \sigma_2\right)\right) \quad ,$$

$$\Delta z_4 = -B\xi_3 - C\theta_3 + \frac{1}{2\zeta}\left(\kappa_3 - \rho_1 + \nu_1\right) \quad ;$$

$$\Delta x_5 = -B\xi_1 - C\theta_1 + \frac{1}{2\zeta}\left(-\kappa_1 - \rho_2 - \nu_2\right) \quad ,$$

$$\Delta y_5 = -B\xi_2 - C\theta_2 + \frac{1}{2\zeta}\left(-\kappa_2 + \rho_1 + \nu_1\right) \quad ,$$

$$\Delta z_5 = -A\theta_3 + \frac{1}{\zeta}\left(-\frac{1}{\sqrt{6}}\,\Delta - \frac{1}{\sqrt{3}}\,\sigma_2\right) \quad ;$$

$$\Delta x_6 = -A\theta_1 + \frac{1}{\zeta}\left(-\frac{1}{\sqrt{6}}\,\Delta - \frac{1}{\sqrt{3}}\,\sigma_1\right) \quad ,$$

$$\Delta y_6 = -B\xi_2 - C\theta_2 + \frac{1}{2\zeta}\left(\kappa_2 - \rho_3 - \nu_3\right) \quad ,$$

$$\Delta z_6 = -B\xi_3 - C\theta_3 + \frac{1}{2\zeta}\left(-\kappa_3 + \rho_2 - \nu_2\right) \quad ;$$

and

$$A = \frac{1}{\varepsilon\zeta}\sqrt{\frac{1}{2}\left(\varepsilon^2 + 2\right)} = \frac{1}{\varepsilon\zeta}\left[\frac{1}{2}\left(\varepsilon^2 + 2\right)\right]^{1/2} \quad ,$$

$$B = \left(2\zeta^2\sqrt{\varepsilon^2 + 2}\right)^{-1} = \left[2\zeta^2\left(\varepsilon^2 + 2\right)^{1/2}\right]^{-1} \quad ,$$

$$C = \left[\varepsilon\zeta\sqrt{\frac{1}{2}\left(\varepsilon^2 + 2\right)}\right]^{-1} = \frac{1}{\varepsilon\zeta}\left[\frac{1}{2}\left(\varepsilon^2 + 2\right)\right]^{-1/2} \quad .$$

Note that the translation mode does not contribute to the relative coordinate. This can be traced to the assumption that all the unit cell atoms move by exactly the same amount in this mode; for k = 0 this is true, but for nonzero k the acoustic mode, which corresponds to the coordinate ζ, will indeed couple to the electron's motion, giving rise to the so-called "deformation potential."

3. CRYSTAL-FIELD INTERACTION

In the phenomenological theory of the crystal field interacting with an electron on a rare-earth ion, the conventional Hamiltonian[22]

$$H = \sum_{nm} B^*_{nm} \sum_i C_{nm}(i) \qquad (1)$$

is frequently used. The B_{nm} are obtained by fitting the experimentally measured energy levels using a suitable set of free-ion wave functions to evaluate the matrix elements of equation (1). The number of B_{nm} in equation (1) is restricted by the symmetry of the site occupied by the rare-earth ion. For the material Cs_2NaRCl_6, the site symmetry of the rare-earth ion is O_h,[23] so that the only independent parameters are B_{40} and B_{60}; the B_{n4} are related by

$$\begin{aligned} B_{44} &= 5B_{40}/\sqrt{70} \ , \\ B_{64} &= -\sqrt{7/2}\, B_{60} \ . \end{aligned} \qquad (2)$$

The spectrum of Er^{3+} in $Cs_2NaErCl_6$ has been analyzed by several workers[15,16,24,25] and the resulting B_{nm} are given in table 1. As can be seen, there is considerable disparity in the reported values of B_{40} and B_{60}. This disparity is due in part to the different identifications made of experimental levels, and in part to use of different free-ion wave functions in calculations.

TABLE 1. REPORTED B_{40} AND B_{60} (cm^{-1}) FOR Er^{3+} IN $Cs_2NaErCl_6$

B_{40}	B_{60}	Ref.
1384	32	24
1368	32	25
1425	153	26
1602	151	27

The oldest, and perhaps the most reliable, crystal-field theory is the point-charge model developed by Bethe[26] in his paper on the spectra of transition metal ions in a solid. In such a model, the constituent ions at $\vec{R}_j$ from the rare-earth ion nucleus have charges eq_j, and the rare-earth electron at $\vec{r}$ interacts with these ions through the Coulomb potential, given by

$$H^0_{CEF} = -e^2 \sum_j \frac{q_j}{|\vec{R}_j - \vec{r}|} \quad . \tag{3}$$

A multipolar expansion of equation (3) can be readily obtained to give

$$H^0_{CEF} = -e^2 \sum_j \sum_{nm} q_j r^n C_{nm}(\hat{r}) C^*_{nm}(\hat{R}_j)/R_j^{n+1} \quad , \tag{4}$$

and if we sum over all the electrons, we may write

$$H^0_{CEF} = \sum_{nm} A^{0*}_{nm} \sum_i r_i^n C_{nm}(\hat{r}_i) \quad , \tag{5}$$

where

$$A^0_{nm} = -e^2 \sum_j q_j C_{nm}(\hat{R}_j)/R_j^{n+1} \quad . \tag{6}$$

These A^0_{nm} are frequently referred to as the multipolar components of the crystal field. The A^0_{nm} have been evaluated for a large number of solids;[27] the results in reference 27 are given in such a way that the q_j in equation (6) can be replaced by effective charges on the ligands. Such a procedure can be used to partially account for covalent complexes in the solid.

Hutchings and Ray[28] recognized that in solids where the ligands occupy sites of sufficiently low symmetry, the point charges of an ionic solid could induce electric dipoles and electric quadrupoles in these ions. These workers did not take into account the fact that these dipoles and quadrupoles also contributed to the electric fields at the sites of low symmetry. The consistent solution for dipoles has been given,[29] and recently the full self-consistent solution through quadrupoles has also been done.* In addition, the corresponding self-consistent solution for arbitrary multipolar moments has recently been published.[20]

For a multipolar moment $Q_{k\beta}(j)$ at $\vec{R}_j$, the A^0_{nm} of equation (6) can be generalized to[20]

$$A^k_{nm} = -e \sum_{j,\beta} (-1)^k \binom{2k+2n}{2k}^{1/2} \langle n(m)k(\beta) | n+k(m+\beta) \rangle \frac{Q^*_{k\beta}(j) C_{n+k,m+\beta}(\hat{R}_j)}{R_j^{n+k+1}} \tag{7}$$

where

$$\binom{2k+2n}{2k} = \frac{(2n+2k)!}{(2k)!(2n)!}$$

*M. Faucher and O. Malta (private communication).

and the quantity in angular brackets is a Clebsch-Gordan coefficient. It should be noted that if k = 0 in equation (7), the result is the same as that of equation (6) if $Q_{00}(j) = eq_j$; the two expressions are consistent. Thus, if the $Q_{kq}(j)$ have been determined, their contribution to the crystal field is given by equation (7).

A further interaction recently considered is the self-induced interaction.[20] This interaction is caused by an electron on the rare earth inducing a multipole moment in a ligand, which then interacts back on the electron. The resultant A_{nm} are given by

$$A_{nm}^{\text{self-induced}} = -e^2 \sum_{\ell,j} \alpha_\ell(j) \frac{(\ell+n)!}{\ell!n!} \left[\frac{2^{n-1}(n!)^2}{(2n)!} - 1\right] \times C_{nm}(\hat{R}_j)/R_j^{2\ell+n+2} \quad . \tag{8}$$

The results of equations (8) and (7) have been used to evaluate the various contributions to A_{nm} for $LaCl_3$,[30] and it is shown that each of these interactions contributes significantly. Although we are here interested in the material $Cs_2NaErCl_6$, we give the results for $LaCl_3$ from Brockhouse[20] in table 2 to illustrate the significance of the contribution to the A_{nm} given by equation (8).

TABLE 2. ELECTROSTATIC CONTRIBUTIONS TO A_{nm} FOR $LaCl_3$

Dipole and quadrupole calculations performed using $\alpha_1 = 1.5$ Å^3 and $\alpha_2 = 3.44$ Å^5

A_{nm}	Point charge[a]	Point dipole[a]	Self-dipole	Self-quadrupole
A_{20}	-2460	3273	-120	-64
A_{40}	-794	-22	135	107
A_{60}	-185	-80	73	77
ReA_{64}[b]	-85	17	-118	-40
ImA_{64}	-63	-39	-99	-34

[a] *From J. B. Gruber, R. P. Leavitt, and C. A. Morrison, J. Chem. Phys. 74 (1981), 2705 (ref 30).*

[b] *In $LaCl_3$ a rotation of the coordinates about the c axis can be performed to make the A_{64} component real. This rotation must be performed after the various contributions to A_{nm} are accounted for.*

The results given in equations (6), (7), and (8) represent a number of interactions of electrons with a rare-earth ion in a solid from the point-charge or point-multipole viewpoint. A number of other possible interactions have been ignored, such as exchange, covalency, configuration interaction, etc.[31] In our discussion of the interactions with the lattice vibrations, we shall restrict ourselves to the interactions given in equations (6), (7), and (8). For an excellent evaluation of the different interactions as of 1971, the reader should consult Newman's article.[31]

4. THE VIBRATIONAL INTERACTION POTENTIAL

The interaction potential we shall consider here is that derived by considering small displacements from the equilibrium configuration of the nucleus and ligands. The particular potential we shall consider in detail is the point charge and its extension to the point-multipole potential. We shall further assume that the various charge distributions are not distorted by their small excursions from equilibrium, i.e., the so-called "rigid-ion" model. An alternative interaction, the superposition model,[31] has recently been considered by Kennedy[32] in his analysis of the effect of an external strain on spectra of rare-earth ions in CaF_2.

Frequently the interaction of an electron on a rare-earth ion with its surroundings is derived from the expansion[33]

$$V = V_o + \sum_k Q_k \frac{\partial V}{\partial Q_k} + \cdots \tag{9}$$

where the Q_k are the normal modes of the lattice. The $\partial V/\partial Q_k$ in equation (9) represent the interaction of the electron with the normal mode Q_k. In general, equation (9) is difficult to use in detailed numerical computation but is excellent for theoretical purposes when one is interested only in the analytical consequences of the effect of vibrations.[33] Since we are interested in numerical values of the strength of the electron-lattice interaction, we shall use a somewhat different expansion, which we present in the following.

Consider a rare-earth ion at the origin, an electron at $\vec{r}$, and a ligand at $\vec{R}_j$ that is displaced by $\vec{s}_j$. The ligand is assumed to have a set of multipole moments Q_{kq}. The electric potential at the electron is given by

$$\phi = \sum_{kq} (-1)^k Q_{kq}(j) \frac{C^*_{kq}(\hat{R}_1)}{R_1^{k+1}} \quad , \tag{10}$$

where $\vec{R}_1 = \vec{R}_j - \vec{r} + \vec{s}_j$. Using the two-center expansion[34] of

$$C^*_{kq}(\hat{R}_1)/R_1^{k+1},$$

we obtain

$$\frac{C^*_{kq}(\hat{R}_1)}{R_1^{k+1}} = \sum_{a\alpha} (-1)^a \binom{2a+2k}{2a}^{1/2} \langle a(\alpha)k(q)|a+k(\alpha+q)\rangle\, s_j^a \times \frac{C_{a\alpha}(\hat{s}_j) C^*_{a+k,q+\alpha}(\hat{R}_2)}{R_2^{a+k+1}}, \tag{11}$$

where $\vec{R}_2 = \vec{R}_j - \vec{r}$. A repeat of the two-center expansion of

$$C^*_{a+k,q+\alpha}(\hat{R}_2)/R_2^{a+k+1}$$

gives

$$\frac{C^*_{a+k,q+a}(\hat{R}_2)}{R_2^{k+a+1}} = \sum_{nm} \binom{2n+2k+2a}{2n}^{1/2} \langle n(m)k+a(q+\alpha)|n+k+a(m+q+\alpha)\rangle \times r^n C_{nm}(\hat{r}) \frac{C^*_{n+k+a,m+q+\alpha}(\hat{R}_j)}{R_j^{n+k+a+1}}. \tag{12}$$

We are interested only in terms linear in the displacement (a = 1 in equation (11)), so that combining equations (12) and (11) into equation (10) gives

$$\phi = -\sum_{\substack{kq \\ \alpha,n,m}} (-1)^k \binom{2k+2}{2}^{1/2} \langle 1(\alpha)k(q)|k+1(q+\alpha)\rangle \binom{2n+2k+2}{2n}^{1/2} \times \langle n(m)k+1(q+\alpha)|n+k+1(m+q+\alpha)\rangle\, r^n C_{nm}(\hat{r}) \times \frac{U_{kq}(j) s_j C_{1\alpha}(\hat{s}_j) C^*_{n+k+1,m+q+\alpha}(\hat{R}_j)}{R_j^{n+k+2}}. \tag{13}$$

The result given in equation (13) is the potential for the ligand at $\vec{R}_j$; the vibrational interaction, V', in the Hamiltonian is given by $-e\phi$, which we write

$$V' = \sum_{nm} \bar{A}^*_{nm} r^n C_{nm}(\hat{r}), \tag{14}$$

by analogy to the interaction of the electrons on a rare-earth ion in the absence of lattice vibrations. The prime on V in equation (14)

indicates that only linear displacements are considered. If we had considered the term a = 0 in equation (11), we would have had the interaction of the electron in the absence of lattice displacement, that is, the crystal-field interaction given by equation (7). Summing equation (13) over all the ligands and comparing with equation (14) gives

$$\bar{A}_{nm} = e \sum_{k,q,a} (-1)^k \binom{2k+2}{2}^{1/2} \binom{2n+2k+2}{2n}^{1/2} \langle 1(\alpha)k(q)|k+1(q+\alpha)\rangle \times \langle n(m)k+1(q+\alpha)|n+k+1(m+q+\alpha)\rangle \times \sum_j Q^*_{kq}(j) \frac{s_j C^*_{1\alpha}(\hat{s}_j) C_{n+k+1,m+q+\alpha}(\hat{R}_j)}{R_j^{n+k+2}} \quad . \tag{15}$$

The result given in equation (15) can be cast into a more useful form by using explicit expressions for the Clebsch-Gordan coefficients to obtain[35]

$$\binom{2k+2}{2}^{1/2} \langle 1(\alpha)k(q)|k+1(q+\alpha)\rangle \binom{2n+2k+2}{2n}^{1/2} \langle n(m)k+1(q+\alpha)|n+k+1(m+q+\alpha)\rangle = \left[\frac{(n+k+1+m+q+a)!(n+k+1-m-q-a)!}{(n-m)!(n+m)!(1-\alpha)!(1+\alpha)!(k-q)!(k+q)!}\right]^{1/2} \quad . \tag{16}$$

Then, from equation (15), we have

$$\bar{A}_{nm} = e \sum_{k,q,\alpha} (-1)^k \left[\frac{(n+k+1+m+q+a)!(n+k+1-m-q-a)!}{(n-m)!(n+m)!(1-\alpha)!(1+\alpha)!(k-q)!(k+q)!}\right]^{1/2} \times \sum_j Q^*_{kq}(j) \frac{s_j C^*_{1\alpha}(\hat{s}_j) C_{n+k+1,m+q+\alpha}(\hat{R}_j)}{R_j^{n+k+2}} \quad , \tag{17}$$

which is the form of the interaction that we find the most convenient to use. For a particular normal mode, the $\hat{s}_j$ have been specified in section 2, and the $Q_{kq}(j)$ will also be considered known. Thus the sum over j given in equation (17) can be performed for any vibrational mode of interest, and the resulting $\bar{A}_{nm}$ for that particular mode can be determined. Thus, the result given in equation (17) is particularly adaptable for calculations using a computer. The $Q_{1q}(j)$ can be found from an appropriate lattice sum and some self-consistent method. The dipole terms (Q_{1q}) have been obtained for a number of solids,[25,36,37]* and in particular for the material Cs_2NaRCl_6[25] for R any of the rare-earth ions. The $\hat{R}_j$ in equation (17) are obtained from the x-ray data, so that with these data the sum given in equation (17) can be coded for computation to cover as many unit cells as is necessary for convergence. In computing the sums, the quantities $s_j C_{1\alpha}(\hat{s}_j)$, $Q_{kq}(j)$, and $\hat{R}_j$ need only be specified for a unit cell, and lattice displacements can then be used

*M. Faucher and O. Malta (private communication).

to cover the complete solid (in the $\vec{K} = 0$ limit). It is also possible to approximately take into account some of the phonon dispersion by replacing $s_j C_{1\alpha}(\hat{s}_j)$ by $s_j C_{1\alpha}(\hat{s}_j) \cos \vec{K}\cdot\vec{R}_j$ and evaluating the sum on j in equation (17) for particular values of $\vec{K}$. However, in the following we shall specialize equation (17) to the particular $(RCl_6)^{-3}$ complex and obtain specific algebraic expressions for $\bar{A}_{nm}$ for each of the modes.

5. THE ELECTRON-VIBRATION INTERACTION FOR $(RCl_6)^{-3}$

As shown in section 2, the vibrational modes of the $(RCl_6)^{-3}$ complex decompose into the following representations of the O_h group (neglecting the translation and rotation modes)

$$\Gamma_1^+(a_{1g}) + 2\Gamma_4^-(t_{1u}) + \Gamma_5^-(t_{2u}) + \Gamma_3^+(e_g) + \Gamma_5^+(t_{2g}) \quad .$$

Here, we are only interested in the vibrationally induced electric-dipole transitions, which are of odd parity (Γ^-). Since the total interaction Hamiltonian must be of even parity, we then require only the odd-parity vibronic modes. That is, we shall discuss only the two modes $\Gamma_4^-(t_{1u})$ and $\Gamma_5^-(t_{2u})$. The latter will be discussed first.

5.1 $\bar{A}_{nm}$ for $\Gamma_5^-(t_{2u})$ Mode

The appropriate vibration for the single Γ_5^- mode is given in figure 4(H). The displacements corresponding to the coordinate κ_3 are

$$\begin{aligned} s_j C_{1\alpha}(\hat{s}_j) &= -z_1 \delta_{\alpha,0} \quad , \qquad \text{for } j = 1 \text{ and } 6 \quad , \\ s_j C_{1\alpha}(\hat{s}_j) &= z_1 \delta_{\alpha,0} \quad , \qquad \text{for } j = 2 \text{ and } 4 \quad , \end{aligned} \tag{18}$$

where z_1 is the displacement of the ligand labeled 1 in figure 2; these displacements follow from the mode equations given in section 2.

The position and multipole moments can all be related to the ligand at 1 by rotations about the z axis. That is,

$$Q^*_{k,q}(2) C_{n+k+1,m+q}(\hat{R}_2) = e^{im\pi/2} Q^*_{k,q}(1) C_{n+k+1,m+q}(\hat{R}_1)$$

with a similar expression for the relation of 6 to 1, which we denote symbolically as

$$(6) = e^{im\pi}(1)$$

and

$$(4) = e^{-im\pi/2}(1) \quad . \tag{19}$$

Using equations (18) and (19) in the sum over α and j in equation (17), we obtain

$$\sum_{\alpha j} s_j C^*_{1\alpha}(\hat{s}_j) Q^*_{kq}(j) C_{n+k+1,m+q}(\hat{R}_j) = -4z_1 Q^*_{kq}(1) C_{n+k+1,m+q}(\hat{R}_1)\delta_{m,4p+2} \quad , \tag{20}$$

with $p = 0, \pm 1, \pm 2 \ldots$

In obtaining the result given in equation (20), we have used the fact that all $|\vec{R}_j|$ have the same value (the x-ray determined distance from the rare-earth ion to the Cl^-). Using the results of equation (20) in equation (17) for the monopole term (for k = 0, $Q_{00}(j) = eq_{c1}$), we obtain the following nonvanishing $\bar{A}_{nm}$:

$$\begin{aligned} \bar{A}_{32}(0) &= K_3\sqrt{12}\, C_{42}(1) \quad , \\ \bar{A}_{52}(0) &= K_5\sqrt{32}\, C_{62}(1) \quad , \\ \bar{A}_{72}(0) &= K_7\sqrt{60}\, C_{82}(1) \quad , \\ \bar{A}_{76}(0) &= K_7\sqrt{28}\, C_{86}(1) \quad , \end{aligned} \tag{21}$$

with

$$K_n = -4e^2 q_{c1} z_1 / R^{n+2} \quad .$$

(K_n will be used for the multiplication factors; in general, its value in each particular case will be given.) Also, we have taken equation (17) as

$$\bar{A}_{nm} = \sum_k \bar{A}_{nm}(k) \quad , \tag{17a}$$

where k represents the multipole moment on the ligand.

For the dipole terms ($Q_{1q}(j)$) the site occupied by the chlorine ion (site 1) has only the components with q = ± 1; using this and the result given in equation (20) in equation (17) gives

$$\begin{aligned} \bar{A}_{32}(1) &= K_3\sqrt{24}\left[\sqrt{14}\, Q^*_{11}\, C_{53}(1) - \sqrt{3}\, Q_{11}\, C_{51}(1)\right] \quad , \\ \bar{A}_{52}(1) &= K_5\sqrt{480}\left[\sqrt{3}\, Q^*_{11}\, C_{73}(1) - Q_{11}\, C_{71}(1)\right] \quad , \\ \bar{A}_{72}(1) &= K_7\sqrt{120}\left[\sqrt{33}\, Q^*_{11}\, C_{93}(1) - \sqrt{14}\, Q_{11}\, C_{91}(1)\right] \quad , \\ \bar{A}_{76}(1) &= K_7\sqrt{168}\left[\sqrt{20}\, Q^*_{11}\, C_{93}(1) - Q_{11}\, C_{91}(1)\right] \quad , \end{aligned} \tag{22}$$

with

$$K_n = +4e^2 z_1 / R^{n+3} \ ,$$

and z_1 is the same as in equation (21).

5.2 $\bar{A}_{nm}$ for $\Gamma_4^-(t_{1u})$ Modes

The appropriate normal modes for $\Gamma_4^-(t_{1u})$ vibration interaction are given by linear combinations of the two vibrations labeled $\vec{\xi}$ and $\vec{\theta}$, shown in figure 4 (E) and (F). Thus, it is appropriate here to discuss the fields associated with the two corresponding $\Gamma_4^-(t_{1u})$ symmetry coordinates. Later we will discuss the selection of the appropriate combinations of these two symmetric functions that form true normal modes of vibration. Also, since the $\bar{A}_{nm}$ for the other two components of these two modes are trivially related, we shall give only the coefficients for the vibrations depicted in figure 4 (E) and (F).

From the figures, the displacements, s_j, of the ligands corresponding to ξ_3 are

$$s_j C_{1\alpha}(\hat{s}_j) = z_1 \delta_{\alpha 0} \ , \qquad \text{for} \quad j = 1, 2, 6, \text{ and } 4 \ ; \tag{23}$$

and

$$s_j C_{1\alpha}(\hat{s}_j) = z_2 \delta_{\alpha 0} \ , \qquad \text{for} \quad j = 3 \text{ and } 5 \ . \tag{24}$$

For the θ_3 mode, we will replace z_1 and z_2 by z_1' and z_2'. The sum on α and j in equation (17) becomes

$$\sum_{\alpha j} s_j C_{1\alpha}(\hat{s}_j) C_{n+1,m+\alpha}(\hat{R}_j) \tag{25}$$
$$= 4z_1 C_{n+1,m}(\hat{R}_1)\delta_{m,4p} + 2z_2 C_{n+1,m}(\hat{R}_3)\delta_{n,2k+1}\delta_{m,0} \ ,$$

where $p = 0, \pm 1, \pm 2 \ldots$ and $k = 0, 1, 2 \ldots$. Using equation (25) in equation (23) results in the following $\bar{A}_{nm}(0)$ for the two modes:

$$\begin{aligned}
\bar{A}_{10}(0) &= 2K_1\left[2C_{20}(1) + \bar{z}_2 C_{20}(3)\right] \ , \\
\bar{A}_{30}(0) &= 2K_3\left[2C_{40}(1) + \bar{z}_2 C_{40}(3)\right] \ , \\
\bar{A}_{50}(0) &= 3K_5\left[2C_{60}(1) + \bar{z}_2 C_{60}(3)\right] \ , \\
\bar{A}_{54}(0) &= 2\sqrt{5}\, K_5\left[C_{64}(1)\right] \ , \\
\bar{A}_{70}(0) &= 4K_7\left[2C_{80}(1) + \bar{z}_2 C_{80}(3)\right] \ , \\
\bar{A}_{74}(0) &= 4\sqrt{3}\, K_7\left[C_{84}(1)\right] \ ,
\end{aligned} \tag{26}$$

where

$$\bar{z}_2 = z_2/z_1 \quad ,$$

$$K_n = 4e^2 q_{c1} z_1 / R^{n+2} \quad .$$

The effective $\bar{A}_{nm}(1)$ for the $\Gamma_4^-(t_{1u})$ modes can be obtained in a similar manner as the $\bar{A}_{nm}(0)$ for this mode. Because of the symmetry of the Cl^- site in Cs_2NaRCl_6 (C_{4v}), the dipoles $\varrho_{1\alpha}(j)$ located at sites 1, 2, 4, and 6 are nonvanishing for $\alpha = \pm 1$ only, while the dipoles at 3 and 5 have $\alpha = 0$ only. From equation (17)--see also equation (17a)--we have

$$\bar{A}_{nm}(1) = \frac{-e}{R^{n+3}} \sum_q \left[\frac{(n+2+m+q)!(n+2-m-q)!}{(n-m)!(n+m)!(1-q)!(1+q)!} \right]^{1/2} \times \sum_j \varrho^*_{1q}(j) s_j C_{10}(\hat{s}_j) C_{n+2,m+q}(\hat{R}_j) \quad . \tag{27}$$

From figure 4 (E) and (F), and the fact that the Cl^- at 1, 2, 4, and 6 are simply related by rotations, it follows that

$$\sum_j{}' \varrho^*_{1q}(j) s_j C_{10}(\hat{s}_j) C_{n+2,m+q}(\hat{R}_j) = 4 z_1 \varrho^*_{1q}(1) C_{n+2,m+q}(1) \delta_{m,4p} \quad , \tag{28}$$

where the prime on the sum means j = 3 and 5 are missing. For j = 5, we have the relation,

$$\varrho^*_{1q}(5) C_{n+2,m+q}(5) = (-1)^{n+1} \varrho^*_{1q}(3) C_{n+2,-m-q}(3)$$

and

$$\varrho_{1q}(3) = \varrho_{10}(3) \delta_{q,0}$$

from the symmetry of the Cl^- site. Thus,

$$\sum_{j=3,5} \varrho^*_{1q}(j) s_j C_{10}(s_j) C_{n+2,m+q}(R_j) = 2 z_2 \varrho^*_{1q}(3) C_{n+2,0}(3) \delta_{m0} \delta_{q0} \delta_{n,2k+1} \quad , \tag{29}$$

where k = 0, 1, 2 . . .

Finally, using equations (28) and (29) in equation (27), we obtain

$$\bar{A}_{10}(1) = K_1\{2\sqrt{6}\,[Q^*_{11}(1)C_{31}(1) + Q_{11}(1)C^*_{31}(1)] + 3\bar{z}_2 Q_{10}(3)C_{30}(3)\} \quad ,$$

$$\bar{A}_{30}(1) = K_3\{4\sqrt{15}\,[Q^*_{11}(1)C_{51}(1) + Q_{11}(1)C^*_{51}(1)] + 10\bar{z}_2 Q_{10}(3)C_{50}(3)\} \quad ,$$

$$\bar{A}_{50}(1) = K_5\{12\sqrt{7}\,[Q^*_{11}(1)C_{71}(1) + Q_{11}(1)C^*_{71}(1)] + 21\bar{z}_2 Q_{10}(3)C_{70}(3)\} \quad ,$$

$$\bar{A}_{54}(1) = K_5\{2\sqrt{30}\,[\sqrt{11}\,Q^*_{11}(1)C_{75}(1) - Q_{11}(1)C_{73}(1)]\} \quad , \qquad (30)$$

$$\bar{A}_{70}(1) = K_7\{24\sqrt{5}\,[Q^*_{11}(1)C_{91}(1) + Q_{11}(1)C^*_{91}(1)] + 36\bar{z}_2 Q_{10}(3)C_{90}(3)\} \quad ,$$

$$\bar{A}_{74}(1) = K_7\{4[\sqrt{273}\,Q^*_{11}(1)C_{95}(1) - 3\sqrt{5}\,Q_{11}(1)C_{93}(1)]\} \quad ,$$

where

$$K_n = -e^2\,4z_1/R^{n+3} \quad .$$

Also, because of the symmetry of the Cl^- site,

$$Q_{1\pm1}(1) = \mp\frac{1}{\sqrt{2}}\,Q_{10}(3) \quad .$$

The results given for the $\bar{A}_{nm}$ in equations (26) and (30) are only for the symmetry coordinates shown in figure 4 (E) and (F). For the true normal modes, we should replace z_1 and z_2 in the above by z_1'' and z_2'', where

$$z_1'' = z_1 \cos\psi + z_1' \sin\psi \quad ,$$
$$z_2'' = z_2 \cos\psi + z_2' \sin\psi \quad , \qquad (31)$$

for the normal modes of vibration for the two $\Gamma_4^-(t_{1u})$ modes. Two values of ψ in equation (31) are determined from the force constants in the vibration Hamiltonian. It can be shown that the effective $\bar{A}_{nm}(k)$ for the two normal modes of the $\Gamma_4^-(t_{1u})$ are

$$\bar{A}''_{nm}(k) = \bar{A}_{nm}(k)\cos\psi + \bar{A}'_{nm}(k)\sin\psi$$

and

$$\bar{A}''_{nm}(k) = -\bar{A}_{nm}(k)\sin\psi + \bar{A}'_{nm}(k)\cos\psi \quad , \qquad (32)$$

where the $\bar{A}_{nm}(k)$ are given by equations (26) or (30) and the $\bar{A}'_{nm}(k)$ are given by the same equations but with z_1 replaced by z_1', etc.

5.3 Computation of $\bar{A}_{nm}(0)$ for $\Gamma_5^-(t_{2u})$ Mode

As was stated earlier, the importance of the vibronic interaction is to mix g and i states with the f states to allow normally forbidden electric-dipole matrix elements of those ions in sites with inversion symmetry. The only vibronics that can contribute to the electric-dipole transition are those with odd parity: Γ_i^-. The reference displacement relative to the rare-earth ion, z_1 in equations (21), (22), (26), and (30) is simply proportional to the amplitude of the normal mode, say Q_k. If we consider transitions where a phonon is created, then

$$\langle 1|Q_k|0\rangle = (\hbar/2\omega_k M_k)^{1/2} \quad , \tag{33}$$

where ω_k is the frequency of the vibronic and M_k is the reduced mass for that mode. For the $\Gamma_5^-(t_{2u})$ mode (referred to as ν_6 elsewhere[15]), the reduced mass for the $(ErCl)^{-3}$ skeleton is simply the mass of the chlorine, and equation (33) gives

$$\langle 1|Q_k|0\rangle = 0.073 \text{ Å} \quad , \tag{34}$$

where we have taken the energy of the $\Gamma_5^-(t_{2u})$ mode as 87 cm^{-1}, as given by Hasan and Richardson.[16] The $C_{nm}(j)$ that occur in the expressions for the $\bar{A}_{nm}(k)$ can be obtained from Karayianis and Morrison,[27] and the values of R can be obtained from the x-ray data. Table 3 gives the results of the calculation using the point-charge contribution, equation (21), for the $\bar{A}_{nm}$, arising from the $\Gamma_5^-(t_{2u})$ mode of vibration. It is interesting to compare the results given in table 3 to the odd-fold crystal-field components of $LiYF_4$, which does not have an inversion center. For $LiYF_4$, $A_{32} = 657 - 667i$, $A_{52} = -2671 - 59i$, $A_{72} = 7 + 14i$, and $A_{76} = 254 + 45i$ (all A_{nm} in units of $cm^{-1}/Å^n$, as in table 3). The magnitude of the A_{nm} for $LiYF_4$ relative to the effective fields due to the vibronic interaction in $Cs_2NaErCl_6$ indicates, at least for the mode $\Gamma_5^-(t_{2u})$, that we should expect the latter to have a much smaller line strength. Using the results of table 3, we calculated the intensities of the $\Gamma_5^-(t_{2u})$ mode for the monopole interaction of Er^{3+} in $Cs_2NaErCl_6$ for all the Er^{3+} levels below 27,000 cm^{-1}. The results of this calculation given in table 4 (p 28) are only for the transition from the Γ_8 ground state to the various upper levels. Thus, the calculations should be compared to experimental data taken at low temperature. In general, for all the multiplets, the intensities of the vibronics are approximately equal to the magnetic intensities. For the $^4I_{15/2} \rightarrow {}^4I_{13/2}$ transition, our calculations agree qualitatively with the calculations of Hasan and Richardson.[16] That is, the vibronic intensity is smaller than the magnetic-dipole intensity and the $\Gamma_8 \rightarrow \Gamma_6$ magnetic-dipole intensity is predicted to be the largest (see

fig. 1, Hasan and Richardson[16]). The calculation for the $^4I_{15/2} \rightarrow {}^4F_{9/2}$ tranisitions indicates that all the ν_6 vibronics have approximately the same intensity as the corresponding magnetic-dipole transitions, and this corresponds to what is observed experimentally (fig. 3, Hasan and Richardson[16]). A detailed comparison of calculated and experimental results will have to wait until the dipole contribution and perhaps the self-induced interactions, equation (8), are included in the effective odd-fold field components.

TABLE 3. POINT-CHARGE CONTRIBUTION TO ODD n $\bar{A}_{nm}(cm^{-1}/\text{Å}^n)$; EFFECTIVE CRYSTAL FIELDS FOR $\Gamma_5^-(t_{2u})$ MODE OF $Cs_2NaErCl_6$[a,b]

Component	Value
$\bar{A}_{32}$	139.08
$\bar{A}_{52}$	-23.755
$\bar{A}_{72}$	3.6372
$\bar{A}_{76}$	2.8996

[a] *The x-ray data were taken from ref 13 (Morss et al, Inorg. Chem. 9 (1970), 1771) with the position of the Cl^-, relative to the Na^+, x = 0.260.*

[b] *From ref 25 (Morrison et al, J. Chem. Phys. 73 (1980), 2580). In the appendix to ref 25, the dipole fields are given for $Cs_2NaNdCl_6$. The formulas necessary to calculate the dipole field for any R^{3+} in Cs_2NaRCl_6 are also given there.*

6. CONCLUSION

The results of the simple calculation of the intensity of the ν_6 vibronics of Er^{3+} in $Cs_2NaErCl_6$ is rather encouraging in that the qualitative agreement with experiment appears good. Certainly the calculations indicate that a further refinement in the theory of the vibrational interaction and the inclusion of an intensity calculation for the two t_{1u} vibrational modes is called for. The calculations here only considered the vibrations of the $(ErCl_6)^{-3}$ complex and therefore are only approximate; further refinements should also be carried out with the use of the results given by Lentz[18] for all of the modes of the unit cell. Such a calculation could easily be carried out using the results of equation (17) for the vibrational-electronic interaction. A considerable amount of experimental data exist for comparison with the calculation for many R^{3+} in Cs_2NaRCl_6. The resulting theory can then be applied to the possibility of constructing a tunable laser using the isomorphic material Rb_2NaRF_6, which is more stable. The theory is also applicable to the development of high-frequency phonon generation (using the lattice modes of Lentz[18]). Further, the theory is applicable to the generation of submillimeter electromagnetic waves by other means such as polaritons and tuning by an external magnetic field. By a slight extension of the theory, the possibility of building a tunable green laser using Ce^{3+} in Rb_2NaYF_6 can be investigated.

TABLE 4. TRANSITIONS FROM Γ_8 OF $^4I_{15/2}$ TO HIGHER LEVELS OF Er^{3+} IN $Cs_2NaErCl_6$

All vibronics are for no phonon ground states

State LSJ	IR	Energy[a] (calc.)	Energy[b] (obs.)	Energy[c] (obs.)	S^{md}	$S^{ed}_{\nu_6}$
$^4I_{15/2}$	Γ_8	0	0	0		
$^4I_{13/2}$	Γ_6	6521	6492	6462	4.57(-6)	6.65(-10)
	Γ_8	6550	6517	6491	2.90(-6)	1.84(-9)
	Γ_7	6568	6532	6517	5.08(-7)	7.95(-10)
	Γ_8	6732	6660	-	2.35(-8)	6.30(-9)
	Γ_7	6735	6683	6627	4.31(-12)	4.20(-9)
$^4I_{11/2}$	Γ_6	10223	[9976]	10160	3.085(-11)	4.980(-10)
	Γ_8	10235	10036	-	8.152(-10)	1.111(-9)
	Γ_7	10325	[10163] (Γ_8)	-	9.649(-10)	2.340(-10)
	Γ_8	10328	10199 (Γ_7)	-	1.957(-9)	9.231(-10)
$^4I_{9/2}$	Γ_8	12336	-	-	2.318(-9)	1.492(-9)
	Γ_8	12460	-	-	2.215(-9)	5.008(-10)
	Γ_6	12511	-	-	4.951(-9)	1.244(-9)
$^4F_{9/2}$	Γ_8	15204	15158	15200	3.269(-9)	5.654(-9)
	Γ_8	15309	15255	-	7.434(-9)	3.254(-9)
	Γ_6	15388	15347	15326	1.734(-9)	1.265(-9)
$^4S_{3/2}$	Γ_8	18341	18276	-	1.990(-9)	7.611(-10)
$^2H_{11/2}$	Γ_8	19144	19020	18968 (Γ_6)	2.326(-9)	1.468(-9)
	Γ_8	19166	19058	19011 (Γ_6)	1.898(-9)	1.953(-9)
	Γ_7	19227	[19143]	19188 (Γ_8)	1.620(-9)	5.185(-9)
	Γ_7	19252	19181	19248 (Γ_8)	9.774(-11)	4.537(-9)
$^4F_{7/2}$	Γ_6	20436	20338	-	3.613(-12)	8.56(-10)
	Γ_6	20494	24437	-	7.620(-11)	1.26(-9)
	Γ_7	20509	20463	20387	8.727(-11)	6.32(-10)
$^4F_{5/2}$	Γ_8	22115	[22038]	-	1.982(-10)	5.41(-10)
	Γ_7	22174	22067 (Γ_6)	-	2.886(-11)	6.55(-11)
$^4F_{3/2}$	Γ_8	22550	22459	-	2.373(-10)	2.10(-10)
$^2G_{9/2}$	Γ_8	24503	24437	-	3.729(-12)	5.357(-10)
	Γ_8	24610	24470	-	5.984(-14)	2.789(-10)
	Γ_6	24650	[24529]	-	6.855(-11)	4.366(-10)
$^4G_{11/2}$	Γ_8	26305	26110	-	1.179(-9)	1.942(-9)
	Γ_8	26380	26193	-	1.490(-9)	2.390(-9)
	Γ_7	26538	26367	-	1.360(-9)	6.631(-9)
	Γ_8	26584	26425	-	1.540(-10)	5.708(-9)

[a] *Calculated using the B_{nm} from Morrison, Leavitt, and Wortman, J. Chem. Phys. 73 (1980), 2580 (ref 25); the centroids have not been adjusted for best fit.*

[b] *Experimental, Hasan and Richardson, Molec. Phys. 45 (1982), 1299 (ref 16); only IR labels that differ from a are listed. The levels in brackets were not observed but were inferred by calculation done in ref 16.*

[c] *Experimental, Jezowska-Trzebiatowska et al, Chem. Phys. 50 (1980), 209 (ref 15); IR are labeled when they disagree with a.*

The numbers in parenthesis in the last two columns are powers of ten.
IR--irreducible representation of the cubic group.
S^{md}--magnetic-dipole strength.
$S^{ed}_{\nu_6}$--electric-dipole strength for ν_6 line.

LITERATURE CITED

(1) G. V. Bukin, S. Yu. Volkov, V. N. Matrosov, B. K. Sevastyanov, and M. Timoshechkin, Kvant. Electron. (Moscow) 5 (1978), 1168; Eng. Transl., Sov. J. Quantum Electron. 8 (1978), 671.

(2) J. C. Walling, H. P. Jenssen, R. C. Morris, E. W. O'Dell, and O. G. Peterson, Opt. Soc. Amer. Meeting (November 1978), San Francisco.

(3) J. C. Walling, H. P. Jenssen, R. C. Morris, E. W. O'Dell, and O. G. Peterson, Opt. Lett. 4 (1979), 182.

(4) D. E. McCumber, Phys. Rev. 134 (1964), A299; see also D. E. McCumber, Phys. Rev. 136 (1964), A954.

(5) J. H. Van Vleck, J. Phys. Chem. 41 (1937), 64.

(6) A. D. Liehr and C. J. Ballhausen, Phys. Rev. 106 (1957), 1161.

(7) A. D. Liehr and C. J. Ballhausen, Ann. Phys. (NY) 3 (1958), 304.

(8) S. Koide and M. H. L. Pryce, Phil. Mag. 3 (1959), 607.

(9) R. A. Satten, J. Chem. Phys. 27 (1957), 286.

(10) R. A. Satten, J. Chem. Phys. 29 (1958), 658; see also Erratum: J. Chem. Phys. 30 (1959), 590.

(11) S. A. Pollack and R. A. Satten, J. Chem. Phys. 36 (1962), 804.

(12) R. A. Satten, D. R. Johnston, and E. Y. Wong, Phys. Rev. 171 (1968), 370.

(13) L. R. Morss, M. Siegal, L. Stenger, and N. Edelstein, Inorg. Chem. 9 (1970), 1771.

(14) C. Cheng and P. B. Dorain, J. Chem. Phys. 65 (1976), 785.

(15) B. Jezowska-Trzebiatowska, W. Ryba-Romanowski, Z. Mazurak, and J. Hanuza, Chem. Phys. 50 (1980), 209.

(16) Zameer-ul Hasan and F. S. Richardson, Molec. Phys. 45 (1982), 1299.

(17) P. J. Cresswell, D. J. Robbins, and A. J. Thomson, J. Lumin. 17 (1978), 311.

(18) A. Lentz, J. Phys. Chem. Solids, 35 (1974), 827.

(19) T. R. Faulkner and F. S. Richardson, Molec. Phys. 39 (1980), 75.

(20) C. A. Morrison, G. F. de Sá, and R. P. Leavitt, J. Chem. Phys. 76, (1982), 3899.

(21) B. N. Brockhouse, Phys. Rev. Lett. 2 (1959), 256.

(22) B. G. Wybourne, Spectroscopic Properties of Rare Earths, Wiley, New York (1965), p. 164.

(23) P. S. Aleonard and C. Pouzet, J. Appl. Cryst. 1 (1968), 113.

(24) H.-D. Amberger, G. G. Rosenbauer, and R. D. Fischer, J. Phys. Chem. Solids 38 (1977), 379.

(25) C. A. Morrison, R. P. Leavitt, and D. E. Wortman, J. Chem. Phys. 73 (1980), 2580.

(26) H. A. Bethe, Ann. Phys. (Leipzig) 3 (1929), 133.

(27) N. Karayianis and C. A. Morrison, Rare Earth Ion-Host Crystal Interaction, 1. Point Charge Lattice Sum in Scheelites, Harry Diamond Laboratories, HDL-TR-1648 (1973). NTIS 776 330.

(28) M. T. Hutchings and D. K. Ray, Proc. Phys. Soc. London 81 (1963), 663.

(29) C. A. Morrison, Solid State Commun. 18 (1976), 153.

(30) J. B. Gruber, R. P. Leavitt, and C. A. Morrison, J. Chem. Phys. 74 (1981), 2705.

(31) D. J. Newman, Adv. Phys. 20 (1971), 197. [In this article, Newman lists a number of interactions ignored here; he also gives the magnitude of these interactions for $LaCl_3$. The result given by Newman for the point charge A_{20} is incorrect; see reference 30 for the correct results.]

(32) R. J. Kennedy, J. Phys. C13 (1980), 5353.

(33) C. J. Ballhausen, Introduction to Ligand Field Theory, McGraw-Hill, New York (1962), p. 187.

(34) B. R. Judd, Angular Momentum Theory for Diatomic Molecules, Academic Press, New York (1975), p. 92.

(35) M. E. Rose, Elementary Theory of Angular Momentum, Wiley, New York (1957).

(36) M. Faucher, J. Dexpert-Ghys, and P. Caro, Phys. Rev. B21 (1980), 3689.

(37) J. Dexpert-Ghys, M. Faucher, and P. Caro, Phys. Rev. B23 (1981), 607.

DISTRIBUTION

ADMINISTRATOR
DEFENSE TECHNICAL INFORMATION CENTER
ATTN DTIC-DDA (12 COPIES)
CAMERON STATION, BUILDING 5
ALEXANDRIA, VA 22314

COMMANDER
US ARMY ARMAMENT RES & DEV COMMAND
ATTN DRDAR-TSS, STINFO DIV
DOVER, NJ 07801

COMMANDER
US ARMY MISSILE & MUNITIONS CENTER
& SCHOOL
ATTN ATSK-CTD-F
ATTN DRDMI-TB, REDSTONE SCI INFO CENTER
REDSTONE ARSENAL, AL 35809

US ARMY MATERIEL SYSTEMS ANALYSIS
ACTIVITY
ATTN DRXSY-MP
ABERDEEN PROVING GROUND, MD 21005

DIRECTOR
US ARMY BALLISTIC RESEARCH LABORATORY
ATTN DRDAR-TSB-S (STINFO)
ABERDEEN PROVING GROUND, MD 21005

DIRECTOR
US ARMY ELECTRONICS WARFARE LABORATORY
ATTN J. CHARLTON
ATTN DELET-DD
FT MONMOUTH, NJ 07703

HQ USAF/SAMI
WASHINGTON, DC 20330

TELEDYNE BROWN ENGINEERING
CUMMINGS RESEARCH PARK
ATTN DR. MELVIN L. PRICE,
MS-44
HUNTSVILLE, AL 35807

ENGINEERING SOCIETIES LIBRARY
ATTN ACQUISITIONS DEPT
345 EAST 4TH STREET
NEW YORK, NY 10017

COMMANDER
US ARMY TEST & EVALUATION COMMAND
ATTN DR. D. H. SLINEY
ATTN TECH LIBRARY
ABERDEEN PROVING GROUND, MD 21005

COMMANDER
ATTN DRSEL-WL-MS, ROBERT NELSON
WHITE SANDS MISSILE RANGE, NM 88002

DIRECTOR
NAVAL RESEARCH LABORATORY
ATTN CODE 2620, TECH LIBRARY BR
ATTN CODE 5554,
DR. S. BARTOLI
ATTN DR. L. ESTEROWITZ
ATTN CODE 5554, R. E. ALLEN
WASHINGTON, DC 20375

DEPARTMENT OF COMMERCE
NATIONAL BUREAU OF STANDARDS
ATTN LIBRARY
ATTN H. S. PARKER
WASHINGTON, DC 20230

DIRECTOR
LAWRENCE RADIATION LABORATORY
ATTN DR. MARVIN J. WEBER
ATTN DR. HELMUT A. KOEHLER
LIVERMORE, CA 94550

CARNEGIE MELLON UNIVERSITY
SCHENLEY PARK
ATTN PHYSICS & EE, DR. J. O. ARTMAN
PITTSBURGH, PA 15213

UNIVERSITY OF MICHIGAN
COLLEGE OF ENGINEERING NORTH CAMPUS
DEPARTMENT OF NUCLEAR ENGINEERING
ATTN DR. CHIHIRO KIKUCHI
ANN ARBOR, MI 48104

COMMANDER
USA RSCH & STD GP (EUR)
ATTN CHIEF, PHYSICS & MATH BRANCH
FPO NEW YORK 09510

DIRECTOR
DEFENSE ADVANCED RESEARCH PROJECTS
AGENCY
1400 WILSON BLVD
ARLINGTON, VA 22209

DIRECTOR
DEFENSE NUCLEAR AGENCY
ATTN TECH LIBRARY
WASHINGTON, DC 20305

DIRECTOR OF DEFENSE RES & ENGINEERING
ATTN TECHNICAL LIBRARY, 3C128
WASHINGTON, DC 20301

OFFICE, CHIEF OF RESEARCH, DEVELOPMENT, &
ACQUISITION
DEPARTMENT OF THE ARMY
ATTN DAMA-ARZ-A, CHIEF SCIENTIST
DR. M. E. LASSER
ATTN DAMA-ARZ-B, DR. I. R. HERSHNER
WASHINGTON, DC 20310

COMMANDER
US ARMY RESEARCH OFFICE (DURHAM)
PO BOX 12211
ATTN DR. ROBERT J. LONTZ
ATTN DR. CHARLES BOGOSIAN
RESEARCH TRIANGLE PARK, NC 27709

COMMANDER
US ARMY MATERIALS & MECHANICS RESEARCH CENTER
ATTN DRXMR-TL, TECH LIBRARY BR
WATERTOWN, MA 02172

COMMANDER
NATICK LABORATORIES
ATTN DRXRES-RTL, TECH LIBRARY
NATICK, MA 01762

COMMANDING OFFICER
USA FOREIGN SCIENCE & TECHNOLOGY CENTER
FEDERAL OFFICE BUILDING
ATTN DRXST-BS, BASIC SCIENCE DIV
CHARLOTTESVILLE, VA 22901

DIRECTOR
NIGHT VISION & ELECTRO-OPTICS LABORATORY
ATTN TECHNICAL LIBRARY
ATTN R. BUSER
ATTN DR. K. K. DEB
ATTN MR. J. PAUL
FT BELVOIR, VA 22060

COMMANDER
ATMOSPHERIC SCIENCES LABORATORY
ATTN TECHNICAL LIBRARY
WHITE SANDS MISSILE RANGE, NM 88002

DIRECTOR
ADVISORY GROUP ON ELECTRON DEVICES
ATTN SECTRY, WORKING GROUP D
201 VARICK STREET
NEW YORK, NY 10013

OFFICE OF NAVAL RESEARCH
ATTN DR. V. O. NICOLAI
ARLINGTON, VA 22217

DEPARTMENT OF MECHANICAL, INDUSTRIAL, & AEROSPACE ENGINEERING
PO BOX 909
ATTN DR. S. TEMKIN
PISCATAWAY, NJ 08854

MASSACHUSETTS INSTITUTE OF TECHNOLOGY
CRYSTAL PHYSICS LABORATORY
ATTN DR. H. P. JENSSEN
ATTN DR. A. LINZ
CAMBRIDGE, MA 02139

NATIONAL OCEANIC & ATMOSPHERIC ADM
ENVIRONMENTAL RESEARCH LABS
ATTN LIBRARY, R-51, TECH RPTS
BOULDER, CO 80302

SETON HALL UNIVERSITY
CHEMISTRY DEPARTMENT
ATTN DR. H. BRITTAIN
SOUTH ORANGE, NJ 07099

OAK RIDGE NATIONAL LABORATORY
ATTN DR. R. G. HAIRE
OAK RIDGE, TN 37830

ARGONNE NATIONAL LABORATORY
9700 SOUTH CASS AVENUE
ATTN DR. W. T. CARNALL
ATTN DR. H. M. CROSSWHITE
ARGONNE, IL 60439

AMES LABORATORY DOE
IOWA STATE UNIVERSITY
ATTN DR. K. A. GSCHNEIDNER, JR.
AMES, IA 50011

ARIZONA STATE UNIVERSITY
DEPT. OF CHEMISTRY
ATTN DR. L. EYRING
TEMPE, AZ 85281

PORTLAND STATE UNIVERSITY
ATTN DR. J. B. GRUBER
PORTLAND, OREGON 92707

PENNSYLVANIA STATE UNIVERSITY
MATERIALS RESEARCH LABORATORY
ATTN DR. W. B. WHITE
ATTN DR. B. K. CHANDRASEKHAR
UNIVERSITY PARK, PA 16802

UNIVERSITY OF VIRGINIA
DEPT OF CHEMISTRY
ATTN DR. F. S. RICHARDSON
CHARLOTTESVILLE, VA 22901

AEROSPACE CORPORATION
PO BOX 92957
ATTN DR. M. BIRNBAUM
ATTN DR. N. C. CHANG
LOS ANGELES, CA 90009

JOHNS HOPKINS UNIVERSITY
DEPT. OF PHYSICS
ATTN PROF. B. R. JUDD
BALTIMORE, MD 21218

KALAMAZOO COLLEGE
DEPT. OF PHYSICS
ATTN PROF. K. RAJNAK
KALAMAZOO, MI 49007

DISTRIBUTION (Cont'd)

US ARMY ELECTRONICS RESEARCH
& DEVELOPMENT COMMAND
ATTN TECHNICAL DIRECTOR, DRDEL-CT

HARRY DIAMOND LABORATORIES
ATTN CO/TD/TSO/DIVISION DIRECTORS
ATTN RECORD COPY, 81200
ATTN HDL LIBRARY, 81100 (3 COPIES)
ATTN HDL LIBRARY, 81100 (WOODBRIDGE)
ATTN TECHNICAL REPORTS BRANCH, 81300
ATTN LEGAL OFFICE, 97000
ATTN CHAIRMAN, EDITORIAL COMMITTEE
ATTN MORRISON, R. E., 13500 (GIDEP)
ATTN LANHAM, C., 00213
ATTN WILLIS, B., 47400
ATTN KARAYIANIS, N., 13200
ATTN KULPA, S., 13300
ATTN LEAVITT, R., 13200
ATTN NEMARICH, J., 13300
ATTN WORTMAN, D., 13200
ATTN SATTLER, J., 13200
ATTN WEBER, B., 13300
ATTN SIMONIS, G., 13200
ATTN WORCHESKY, T., 13200
ATTN TOBIN, M., 13200
ATTN DROPKIN, H., 13200
ATTN CHIEF, 00210
ATTN CHIEF, 13000
ATTN CHIEF, 15000
ATTN MORRISON, C., 13200 (10 COPIES)
ATTN CROWNE, F., 13200 (10 COPIES)

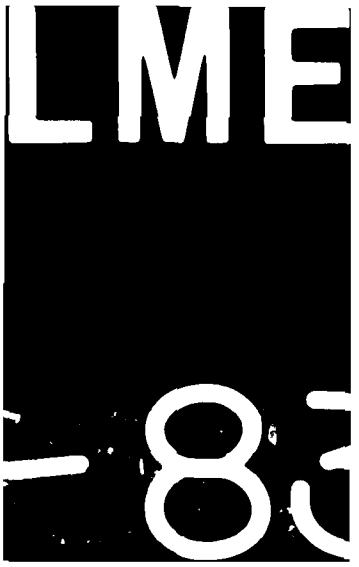
LME